Environmental Science Processes & Impacts

ROYAL SOCIETY OF CHEMISTRY

PAPER

View Article Online
View Journal | View Issue



Check for updates

Cite this: *Environ. Sci.: Processes Impacts*, 2020, **22**, 1084

# Quantitative measures of *myo*-$IP_6$ in soil using solution $^{31}P$ NMR spectroscopy and spectral deconvolution fitting including a broad signal†

Jolanda E. Reusser, *[a] René Verel, [b] Emmanuel Frossard[a] and Timothy I. McLaren [a]

Received 24th October 2019
Accepted 4th March 2020

DOI: 10.1039/c9em00485h

rsc.li/espi

Inositol phosphates, particularly *myo*-inositol hexakisphosphate (*myo*-$IP_6$), are an important pool of soil organic phosphorus (P) in terrestrial ecosystems. To measure concentrations of *myo*-$IP_6$ in alkaline soil extracts, solution $^{31}P$ nuclear magnetic resonance (NMR) spectroscopy is commonly used. However, overlap of the NMR peaks of *myo*-$IP_6$ with several other peaks in the phosphomonoester region requires spectral deconvolution fitting (SDF) to partition the signals and quantify *myo*-$IP_6$. At present, two main SDF approaches are in use; the first fits a Lorentzian/Gaussian lineshape to the *myo*-$IP_6$ peaks directly to the baseline without an underlying broad signal, and the second fits a Lorentzian/Gaussian lineshape to the *myo*-$IP_6$ peaks simultaneously with an underlying broad peak. The aim of this study was to compare the recovery of added *myo*-$IP_6$ to soil extracts using both SDF procedures for six soil samples of diverse origin and differing concentrations of organic P (112 to 1505 mg P per $kg_{soil}$). The average recovery of total added *myo*-$IP_6$ was 95% (SD 5) and 122% (SD 32) using SDF with and without an underlying broad signal, respectively. The recovery of individual peaks of *myo*-$IP_6$ differed, most notably, the C5 phosphate peak of *myo*-$IP_6$ was overestimated by up to 213% when a broad peak was not included in SDF. Based on the SDF procedure that includes a broad peak, concentrations of *myo*-$IP_6$ ranged from 0.6 to 90.4 mg P per $kg_{soil}$, which comprised 1–23% of total phosphomonoesters. Our results demonstrate that the SDF procedure with an underlying broad signal is essential for the accurate quantification of *myo*-$IP_6$ in soil extracts.

### Environmental significance

In terrestrial ecosystems, *myo*-inositol hexakisphosphate (*myo*-$IP_6$) is considered to be a major pool of organic phosphorus (P) in soil. However, there is disagreement in the literature on how to accurately measure *myo*-$IP_6$ in soil using solution $^{31}P$ nuclear magnetic resonance (NMR) spectroscopy. We provide new insights on the use of solution $^{31}P$ NMR spectroscopy followed by spectral deconvolution fitting for the quantitative measurement of *myo*-$IP_6$ in soil extracts. Accurate quantification of *myo*-$IP_6$ is essential for understanding its transformation in soil and hence availability for living organisms as well as its potential contribution to P movement into aquatic ecosystems.

## 1. Introduction

Phosphorus (P) is an essential macronutrient for all living organisms, which is primarily sourced from the soil environment. It is estimated that between 20 and 80% of the total P ($P_{tot}$) in soil exists in an organic form.[1,2] A major pool of identifiable organic P ($P_{org}$) in soil is that of inositol phosphates (IP), of which the *myo* stereoisomer of inositol hexakisphosphate (*myo*-$IP_6$) is the most abundant.[3,4] Studies have reported that pools of *myo*-$IP_6$ comprise on average one third of the total $P_{org}$ in soil.[5] The mechanism for its accumulation in soil is thought to be due to its high binding affinity to aluminum and iron (hydro-)oxides.[6]

Solution $^{31}P$ nuclear magnetic resonance (NMR) spectroscopy has been used since 1980 to identify the chemical nature of $P_{org}$ in soil extracts.[7,8] The majority of P (~80%) in NaOH soil extracts is detected in the phosphomonoester region (organic moiety-O-$PO_3$) of the NMR spectrum.[5] However, due to many overlapping signals in this region, spectral deconvolution fitting (SDF) procedures are required to partition the NMR signal.[9] The two main SDF approaches applied to soil extracts are that of Turner *et al.*, (2003)[10] or modifications thereof,[11] and Bünemann *et al.*, (2008)[12] or modifications thereof.[13]

[a]*Department of Environmental Systems Science, Group of Plant Nutrition, ETH Zurich, Eschikon 33, CH-8315 Lindau, Switzerland. E-mail: jolanda.reusser@usys.ethz.ch*
[b]*Department of Chemistry and Applied Biosciences, Laboratory of Inorganic Chemistry, ETH Zurich, Vladimir-Prelog-Weg 1-5/10, CH-8093 Zurich, Switzerland*

† Electronic supplementary information (ESI) available. See DOI: 10.1039/c9em00485h

Turner *et al.*, (2003)[10] were the first to propose a SDF procedure that could partition the NMR signal within the phosphomonoester region and quantify *myo*-$IP_6$ in soil extracts. The SDF procedure was carried out using the Bruker WinNMR program, and involved fitting a series of sharp signals from the peak maxima of *myo*-$IP_6$ to the baseline of the spectra. The procedure was applied to 29 soils under grassland in the United Kingdom and the authors tested the efficacy of the procedure by calculating the recovery of added *myo*-$IP_6$ in a 1 M NaOH solution containing a mixture of $P_{org}$ compounds. The authors reported that the recovery of added *myo*-$IP_6$ was on average 102%. However, a limitation of this study was that recoveries of added *myo*-$IP_6$ were determined in non-soil extracts.

In contrast, Bünemann *et al.*, (2008)[12] later proposed a SDF for the quantification of $P_{org}$ compounds (*e.g. myo*-$IP_6$) that involved fitting a broad feature in the phosphomonoester region, which was then subtracted from the original NMR spectrum and then the overlaying sharp signals were fitted. The authors hypothesized that the broad signal was caused by phosphomonoesters in large and complex molecules, which was later confirmed by McLaren *et al.*, (2015)[14] and McLaren *et al.*, (2019).[13] Bünemann *et al.*, (2008)[12] did not describe the SDF procedure in detail or test its efficacy at the time. However, Doolette *et al.*, (2010)[15] compared the two SDF procedures (with and without a broad signal) to quantitatively recover *myo*-$IP_6$, which was added to a soil extract. The authors reported that the concentration of *myo*-$IP_6$ was overestimated by 54% when a broad signal was not included. Doolette *et al.*, (2011)[16] later explained the SDF procedure in more detail. A limitation of this study was that the recovery of added *myo*-$IP_6$ was only tested on one soil extract. In addition, both SDF methods were not able to identify the recovery of the four individual peaks of *myo*-$IP_6$ due to poor spectral resolution.

A plethora of studies have been carried out since 2003 to identify the chemical nature of soil $P_{org}$ using solution $^{31}P$ NMR spectroscopy and SDF procedures.[8] Despite this, there has been no detailed assessment on the efficacy of the two main SDF procedures, which has major consequences for how we understand the composition of soil $P_{org}$. The implicit assumption of the SDF procedure without a broad signal is that the phosphomonoester region is comprised of an array of sharp peaks (*e.g. myo*-$IP_6$) with very similar linewidths, which are presumably from small organic molecules.[17,18] In contrast, the implication of the SDF procedure with a broad signal is that it interprets the phosphomonoester region as comprised of a broad signal, which is considered to be $P_{org}$ in the form of large molecular structures and associated with the soil organic matter (SOM),[13,14] and in addition an array of sharp peaks from small organic molecules containing P. It is also important to reconcile these views with previous studies using non-NMR techniques, which often reported large concentrations of $P_{org}$ in large molecular weight fractions.[14,19]

The aim of this study was to assess the efficacy of the two SDF procedures to quantitatively determine *myo*-$IP_6$ in soil extracts. *myo*-Inositol hexakisphosphate was chosen because it can be easily detected in $^{31}P$ NMR spectra on soil extracts as four distinct peaks in a 1 : 2 : 2 : 1 ratio. This ratio is caused by the chemical structure of *myo*-$IP_6$ (see Fig. SI-1 in the ESI†), with the two phosphate groups bound to the C1 and C3 carbon nuclei of the inositol ring being chemically equivalent, and therefore exhibiting the same chemical shift. This is similarly the case for the phosphate groups bound to the C4 and C6 carbon nuclei. The phosphate groups bound to C5 and C2 have distinct chemical environments caused by the conformation of the molecule. The combined four peaks associated with the phosphate groups of *myo*-$IP_6$ can be used to probe a relatively wide chemical shift range in the phosphomonoester region of the $^{31}P$ NMR spectrum using a single compound.

## 2. Materials and methods

### 2.1. Soil collection and preparation

Six soil samples were collected from the upper horizon of soil profiles including different soil types and land use systems across four countries. We included soils that covered a wide diversity of organic P contents and soil properties: two Cambisols (S3 and S6) and a Gleysol (S5) from Switzerland, a Ferralsol (S1) from Colombia, a Cambisol (S4) from Germany, and a Vertisol (S2) from Australia.[20] Soil S1 was collected in 1997 from the 0–20 cm soil layer of the improved grassland treatment of the long-term Culticore field experiment at the Carimagua Research Station in Colombia.[21] Soil S2 was collected in 2017 from the 0–15 cm soil layer of a field under cropping from southern Queensland, Australia. The site has been under cultivation for the past 25 years and prior to this was shrubland containing sparse *Eucalyptus camaldulensis* L. and native grasses. Soil S3 was collected in 2017 from the 0–20 cm soil layer of a cultivated field, but was under grassland for more than 6 years prior. Soil S4 was collected in 2014 from the 0–7 cm topsoil layer of a beech forest in Bad Brückenau, Germany, as described in Bünemann *et al.*, (2016).[22] Soil S5 was collected in 2017 from the 0–10 cm soil layer of a drained marshland, which has been under grassland for more than 20 years, near Lucerne, Switzerland. Sample S6 was collected in 2013 from the 0–20 cm soil layer from an unfertilized border strip of a cultivated field in Rümlang, Switzerland.[23]

Background information on the studied sites, and some chemical and physical properties of the soils, are reported in Table 1. Soils S3, S4 and S5 were passed through a 5 mm sieve and dried at 60 °C for 5 days. Soils S1 and S6 were received dried and sieved at <2 mm, whereas S2 was received dried (at 40 °C for 2 days) and ground at <2 mm. In order to include soils with a diversity of organic P contents and soil properties, soils were sourced from the field in Switzerland and from previous studies.[21–23] Consequently, there were small differences in soil preparation among soils used in this study, which may slightly affect soil P extraction. Nevertheless, these differences will not affect the application of SDF procedures to the resultant NMR spectra for the quantification of added *myo*-$IP_6$ in soil extracts. Concentrations of total carbon ($C_{tot}$) and nitrogen ($N_{tot}$) in soil were measured using combustion of 50 mg ground soil weighed into tin foil capsules (vario PYRO cube®, Elementar Analysesysteme GmbH). Concentrations of 0.5 M $H_2SO_4$ extractable $P_{tot}$ and $P_{org}$ in soil were measured using the ignition-$H_2SO_4$

Table 1 Some background information on the sites and some chemical and physical properties of the soils reported in this study

| Parameter | Unit | S1 | S2 | S3 | S4 | S5 | S6 |
|---|---|---|---|---|---|---|---|
| Soil type | — | Ferralsol | Vertisol | Cambisol | Dystric skeletic Cambisol | Gleysol | Calcaric Cambisol |
| Country | — | Colombia | Australia | Switzerland | Germany | Switzerland | Switzerland |
| Coordinates of sampling | — | 4°30′ N/71°19′ W | 27°52′ S/151°37′ E | 46°55′ N/7°36′ E | 50°21′ N/9°55′ E | 47°05′ N/8°06′ E | 47°26′ N/8°31′ E |
| Elevation | m ASL | 150 | 402 | 748 | 800 | 612 | 443 |
| Sampling depth | cm | 0–20 | 0–15 | 0–20 | 0–7 | 0–10 | 0–20 |
| Land use | — | Pasture | Arable | Pasture | Forest | Pasture | Arable |
| $C_{tot}$ | g C per $kg_{soil}$ | 26.7 | 23.9 | 21.0 | 90.3 | 148.3 | 27.6 |
| $N_{tot}$ | g N per $kg_{soil}$ | 1.7 | 1.9 | 2.3 | 6.6 | 10.9 | 2.5 |
| pH in $H_2O$ | — | 3.6 | 6.1 | 5.1 | 3.6 | 5.0 | 7.7[a] |

[a] Meyer *et al.*, (2017).[23]

method of Saunders and Williams (1955)[24] as described in Kuo (1996).[25] Total concentrations of soil P were determined by X-ray fluorescence spectroscopy (SPECTRO XEPOS ED-XRF, AMETEK®) using 4.0 g of ground soil sample mixed with 0.9 g of wax (CEREOX Licowax, FLUXANA®). The XRF instrument was calibrated using commercially available reference soils. Soil pH was measured in $H_2O$ at a soil to solution ratio of 1 : 2.5 (w/w) with a glass electrode.

### 2.2. Extraction of soil organic P

Concentrations of $P_{org}$ were determined based on the method of Cade-Menun *et al.*, (2002).[26] Briefly, 3.0 g of soil was extracted with 30 mL of 0.25 M NaOH + 0.05 M $Na_2EDTA$. Soil extracts were shaken for 16 h on a horizontal shaker at 150 rpm at 24 °C, centrifuged for 10 min at 4643*g*, and then the supernatant passed through a Whatman no. 42 filter paper. A 20 mL aliquot of the filtrate was frozen at −80 °C and then lyophilized prior to NMR analysis. This resulted in 420 to 782 mg of lyophilized material across all soils. Concentrations of $P_{tot}$ in the remaining filtrates were measured using inductively coupled plasma-optical emission spectrometry (ICP-OES). Concentrations of molybdate reactive P (MRP) were measured using the malachite green method of Ohno and Zibilske (1991).[27] The difference between $P_{tot}$ and MRP in NaOH-EDTA filtrates is molybdate unreactive P (MUP), which is largely considered to be $P_{org}$,[28] but may also include a small proportion of condensed phosphates (*e.g.* pyrophosphate).[29]

### 2.3. Preparation of lyophilized material for solution $^{31}$P NMR spectroscopy

Preparation of lyophilized material for solution $^{31}$P NMR spectroscopy was based on a modification of the methods as reported in Vincent *et al.*, (2013)[30] and Spain *et al.*, (2018).[31] Briefly, 120 mg of lyophilized material was weighed into 1.5 mL microcentrifuge tubes and then a 600 μL aliquot of 0.25 M NaOH + 0.05 M $Na_2EDTA$ solution was added. The solution was briefly vortexed and then allowed to rest overnight in order for complete hydrolysis of RNA and phospholipids.[32–35] This is because the hydrolysis products of RNA (RNA mononucleotides[34]) and phospholipids (α- and β-glycerophosphate[32]) generate peaks in the phosphomonoester region.[32,35] The microcentrifuge tubes were then centrifuged at 10 621*g* for 15 min, and a 500 μL aliquot of the supernatant was transferred to another 1.5 mL microcentrifuge tube, which then received a 25 μL aliquot of a 0.03 M methylenediphosphonic acid (MDP) standard in $D_2O$ (Sigma-Aldrich, product no. M9508) and a 25 μL aliquot of sodium deuteroxide (NaOD) at 40% (w/w) in $D_2O$ (Sigma-Aldrich, product no. 372072). The solution was briefly vortexed and then transferred to 5 mm NMR tubes for analysis.

Subsequent NMR analyses of samples S4 and S5 revealed considerable line-broadening of all peaks in the NMR spectra, which might have been caused by high sample viscosity. Therefore, the preparation of lyophilized material was repeated for these samples but at a wider ratio, as recommended by Cade-Menun and Liu (2014).[8] For these samples, 80 mg of lyophilized material was dissolved in 600 μL of 0.25 M NaOH +

 

0.05 M $Na_2EDTA$ solution, and then prepared as previously described. This overcame the issue and resulted in high resolution NMR spectra.

### 2.4. Solution $^{31}$P NMR spectroscopy

All NMR analyses were carried out with a Bruker Avance IIIHD 500 MHz NMR spectrometer equipped with a 5 mm liquid-state Prodigy™ CryoProbe (Bruker Corporation; Billerica, MA) at the NMR facility of the Laboratory of Inorganic Chemistry (Hönggerberg, ETH Zürich). Solution $^{31}$P NMR spectra were acquired using a $^{31}$P frequency of 202.5 MHz, with gated broadband proton decoupling and 90° pulses (duration of 12 μs) for excitation. Careful shimming of the samples resulted in a spectral resolution of <0.1 Hz. The recycle delay of each sample was set based on an inversion recovery experiment.[36] Briefly, the spin–lattice relaxation times ($T_1$) were calculated from 10 separate experiments with increasing $\tau$ values, the time period between the applied pulses in the inversion recovery sequence. Each spectrum was obtained with the collection of 24 scans and a recycle delay of 5 s. Total duration of the inversion recovery experiment for each sample was 56 min. The recycle delay for each sample was calculated by multiplying the longest $T_1$ value from the inversion recovery experiment by five. This resulted in recycle delays ranging from 6.7 to 31.0 s across all soils. The number of scans was set to 1024 or 4096, depending on the signal to noise ratio of the obtained spectrum.

### 2.5. Processing of NMR spectra

Spectral processing involved Fourier transformation, phase correction and baseline adjustment using the TopSpin® software of Bruker (Version 3.5 pl 7, Bruker Corporation; Billerica, MA). All NMR spectra were processed with an exponential line-broadening of 0.6 Hz. Since the concentration of added MDP is known, its integral (net peak area) is directly proportional to that of all other NMR signals.[16] Therefore, quantification of P species in NMR spectra was carried out based on spectral integration.[37] In general, integral regions included: (1) phosphonates, in particular the added MDP (δ 16.9 to 16.3 ppm), which includes its two carbon satellite peaks (at δ 16.96 and 16.36 ppm), 2-aminoethylphosphonic acid (δ 19.8 to 19.6 ppm), unknown phosphonate 1 (δ 19.3 to 19.2 ppm), unknown phosphonate 2 (δ 18.3 to 18.1 ppm) and unknown phosphonate 3 (δ 16.5 to 16.4 ppm); (2) the combined orthophosphate and phosphomonoester region (δ 6.0 to 3.0 ppm); (3) phosphodiesters, in particular unknown phosphodiester 1 (δ 2.5 to 2.2 ppm), unknown phosphodiester 2 (δ 0.6 to 0.5 ppm), DNA (δ −0.7 to −1.4 ppm) and unknown phosphodiester 3 (δ −2.3 to −2.4 ppm); and (4) pyrophosphate (δ −4.8 to −5.4 ppm). These integral regions are highlighted in Fig. SI-3 in the ESI.† Due to overlapping signals in the orthophosphate and phosphomonoester region, SDF was needed to partition the NMR signals within this region.

### 2.6. Deconvolution fitting procedures

Two spectral deconvolution fitting approaches were applied to the orthophosphate and phosphomonoester region. The first approach involved fitting all identifiable sharp peaks (*i.e.* distinguishable from the noise of the spectrum) to the baseline of the spectra, which is based on the method of Turner *et al.*, (2003).[38] The second approach involved fitting all identifiable sharp signals and simultaneously an underlying broad signal in the phosphomonoester region, which has

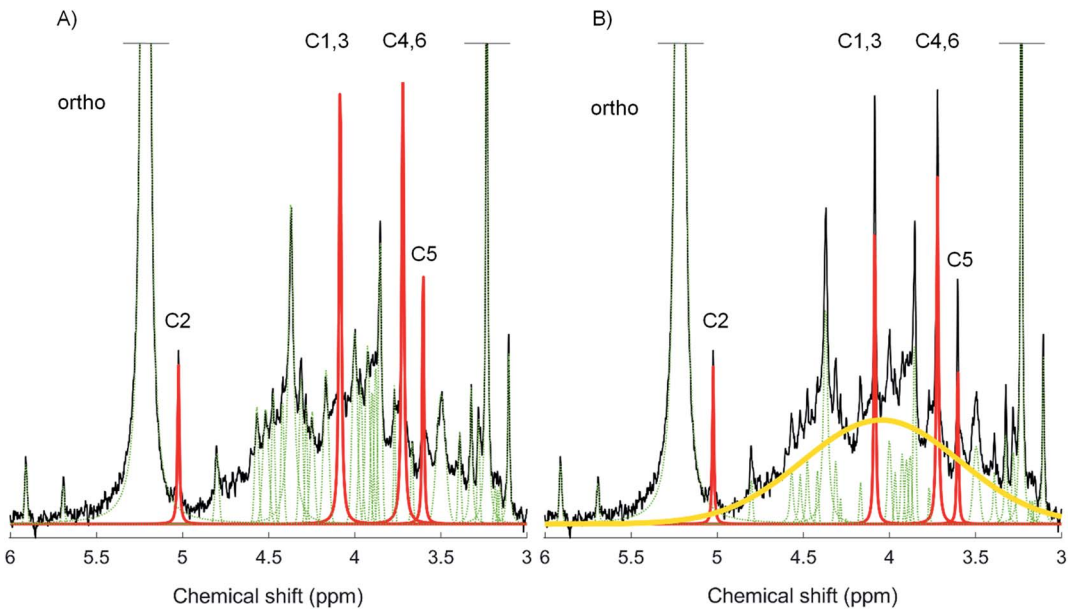


Fig. 1 Solution $^{31}$P NMR spectrum of 0.25 M NaOH + 0.05 M EDTA soil extract S6 (black). Graphical representation of the two spectral deconvolution fitting approaches without (A) and with an underlying broad signal (B). All fitted peaks are illustrated; the broad peak (yellow) and the four *myo*-$IP_6$ peaks (red) have been highlighted. In addition, the phosphate groups bound to carbons C1–6 of *myo*-$IP_6$ and also that of the orthophosphate (ortho) peak, have been identified.

been described in McLaren *et al.*, (2019),[13] and is based on the method of Bünemann *et al.*, (2008).[17] We used MATLAB® R2017a (The MathWorks, Inc.) scripts containing a non-linear optimization algorithm for the SDF of the NMR spectra. Fig. 1 shows a graphical representation of the two deconvolution fitting procedures used in this study (peak assignment according to[16]). For both SDF procedures, a Lorentzian or Gaussian lineshape model was selected for each peak based on a visual assessment of the most optimized fit and calculated residuals. In general, a Lorentzian lineshape was used to fit the broad signal, signals of *myo*-$IP_6$ and orthophosphate, whereas a Gaussian lineshape was used to fit the remaining sharp signals, which were generally of lower signal intensity. Each of the identifiable sharp peaks were fitted between an upper and lower bound on both their linewidths at half height and their peak positions at highest intensity. The same was true for the peak position of the underlying broad signal and its linewidth at half height. The upper and lower bound for both parameters of the broad signal being set to $\delta$ 3.8 ppm and $\delta$ 4.5 ppm, and from 19 Hz to 293 Hz, respectively. Within these visually assessed boundaries, all signals (including the underlying broad signal) were fitted by the non-linear optimization algorithm. The residues of all fitted spectra are plotted in Fig. SI-4 and SI-5 in the ESI.† The goodness of fit parameters of the SDF including the Root-mean-square fitting error and $R^2$ (coefficient of determination) are listed in Table SI-1 (ESI†). Table SI-1† also includes the results of a reduced $Chi^2$-test in MATLAB® with the fitted peaks and the according residuals (chemical shift range $\delta$ 5.2 to 3.0 ppm). We carried out the $Chi^2$-test in order to determine if an overfitting of the spectra occurred ($Chi^2 < 1$). Briefly, the results ($Chi^2 > 1$) show that there was no overfitting of the spectra using both SDF approaches, and that the $Chi^2$ values of the SDF approach with a broad signal were closer to 1 than without a broad signal, which suggests the former approach is a better fit of the spectra. Furthermore, we carried out the Bootstrap sampling function of MATLAB® ($n = 100$) for all peaks within the given boundaries of the peak positions, the area and linewidths at half height. The resulting means of the peak position and linewidths at half height including the standard deviations for the broad signal are listed in Table SI-2 in the ESI.† The calculated standard deviations were very low for all three parameters, indicating a good fit of the broad peak within the given boundaries.

### 2.7. Spiking experiment

The two deconvolution fitting procedures were assessed by determining the recovery of a known amount of added *myo*-$IP_6$ to soil extracts. After NMR analysis of the unspiked soil extract, a 10 μL aliquot of a 5.5 mM *myo*-$IP_6$ standard in $D_2O$ was added to all soil extracts except for soil S5 (Sigma-Aldrich, product no. P5681). For sample S5, a 10 μL aliquot of a 11 mM *myo*-$IP_6$ standard in $D_2O$ was added. The aim was to add *myo*-$IP_6$ at a concentration that would result in an increase of peak intensity of approximately 3-times the peak intensity in unspiked extracts.[32] The NMR tube was then sealed with parafilm, inverted several times, and then allowed to rest prior to NMR analysis. The NMR analysis parameters on the spiked soil extract were the same as that carried out on unspiked extracts. Similarly, spectral processing and quantification were carried out as previously described. The recovery of added *myo*-$IP_6$ was calculated using eqn (1).

$$\text{Recovery of added } myo\text{-IP}_6(\%) = \frac{A(\text{mg P per l}) - B(\text{mg P per l})}{C(\text{mg P per l})} \times 100 \quad (1)$$

where $A$ refers to the concentration of *myo*-$IP_6$ in the spiked soil extract, $B$ to the concentration of *myo*-$IP_6$ in the unspiked extract and $C$ to the concentration of the added *myo*-$IP_6$. Solution $^{31}P$ NMR recovery of the phytate standard revealed impurities, therefore $C$ represents the actual concentration of *myo*-$IP_6$ in the standard (see Fig. SI-2 in the ESI†).

### 2.8. Statistical analyses and graphics

All graphics were created using MATLAB® R2017a (The MathWorks, Inc.). All statistical analyses were carried out using Microsoft® Excel 2016. This included calculating the mean values and standard deviations (SD) of the added *myo*-$IP_6$

Table 2 Total soil phosphorus ($P_{tot}$) as measured by X-ray fluorescence (XRF) spectroscopy, and pools of extractable P using the ignition-$H_2SO_4$ extraction technique of Saunders and Williams (1955)[24] and the NaOH-EDTA extraction technique of Cade-Menun *et al.*, (2002).[26] The percentage of extractable P to that of $P_{tot}$ in soil as measured by XRF is shown in parentheses

| | XRF | Ignition-$H_2SO_4$ extraction | NaOH-EDTA extraction | | |
|---|---|---|---|---|---|
| Soil | $P_{tot}$, mg P per $kg_{soil}$ | $P_{org}$, mg P per $kg_{soil}$ (%) | $P_{tot}$, mg P per $kg_{soil}$ (%) | MRP[a], mg P per $kg_{soil}$ (%) | MUP[b], mg P per $kg_{soil}$ (%) |
| S1 | 320 | 109 (34) | 160 (50) | 67 (21) | 93 (29) |
| S2 | 1726 | 143 (8) | 484 (28) | 351 (20) | 133 (8) |
| S3 | 2553 | 729 (29) | 863 (34) | 323 (13) | 540 (21) |
| S4 | 3841 | 1377 (36) | 1850 (48) | 525 (14) | 1326 (35) |
| S5 | 2913 | 939 (32) | 1490 (51) | 610 (21) | 880 (30) |
| S6 | 1724 | 430 (25) | 510 (30) | 128 (7) | 382 (22) |

[a] Molybdate reactive P (MRP) based on the malachite green method of Ohno and Zibilske (1991).[27] [b] The difference between $P_{tot}$ and MRP is molybdate unreactive P (MUP), which is considered to be $P_{org}$.

 

Table 3 Relative concentrations of P classes determined by solution $^{31}$P NMR spectroscopy as percentage (%) of total P in NaOH-EDTA soil extracts. Chemical shift regions were attributed to P species according to peak positions in spectra

| Soil | Phosphonates[a] ($\delta$ 19.8 to 16.5 ppm) | Orthophosphate ($\delta$ 5.5 to 5.0 ppm) | P-monoester ($\delta$ 6.0 to 3.0 ppm) | P-diesters ($\delta$ 2.5 to −2.4 ppm) | Pyrophosphates ($\delta$ −4.8 to −5.3 ppm) |
|---|---|---|---|---|---|
| S1 | 1.0 | 55.0 | 37.0 | 5.1 | 1.9 |
| S2 | 1.0 | 85.0 | 13.3 | 0.0 | 0.7 |
| S3 | 0.2 | 50.4 | 47.8 | 0.4 | 1.2 |
| S4 | 1.5 | 46.7 | 47.7 | 2.9 | 1.3 |
| S5 | 0.0 | 48.5 | 45.3 | 3.3 | 2.9 |
| S6 | 0.2 | 51.1 | 46.9 | 0.0 | 1.8 |

[a] The added methylenediphosphonic acid (MDP) standard is not included.

recovery across the six soil samples. The NMR observability was calculated by comparing the concentration of $P_{tot}$ as detected by NMR with that measured by ICP-OES,[16,39] which ranged from 52 to 89% (on average of 68%) across all soils.

# 3. Results

## 3.1. Pools of soil P

Concentrations of $P_{tot}$ in soil using XRF ranged from 320 to 3841 mg P per $kg_{soil}$ (Table 2). Concentrations of $P_{tot}$ in NaOH-EDTA extracts comprised 28 to 51% of the $P_{tot}$ in soil as measured by XRF. Concentrations of $P_{org}$ using the ignition-$H_2SO_4$ extraction technique ranged from 143 to 1377 mg P per $kg_{soil}$. The concentration of $P_{org}$ in NaOH-EDTA extracts ranged from 93 to 1326 mg P per $kg_{soil}$, which comprised 8 to 35% (an average value of 24%) of the total soil P using XRF.

## 3.2. Solution $^{31}$P NMR spectra of soil extracts

The majority of NMR signals occurred in the orthophosphate and phosphomonoester region ($\delta$ 6.0 to 3.0 ppm), which comprised on average 96% of total NMR signal (Table 3). In general, the peak of greatest intensity across all soils was that of orthophosphate (apart from the added MDP). The largest pool of $P_{org}$ as determined by the integral over the various regions of peaks was that of phosphomonoesters, which accounts on average for 94% of the total NMR signal arising from organic forms. Concentrations of phosphomonoesters range from 36.3 to 501.1 mg P per $kg_{soil}$. The remaining NMR signal is distributed between phosphodiesters, pyrophosphates and phosphonates.

The phosphomonoester region comprised of two main spectral features based on a visual assessment; the presence of (i) 18 to 47 sharp signals, and (ii) an underlying broad signal. The four peaks of *myo*-$IP_6$ were observed in the NMR spectra of all soils except in soil S2, in which only the C1,3 and C4,6 peaks could be clearly identified due to the low initial concentration of *myo*-$IP_6$. In all soils, the C2 peak of *myo*-$IP_6$ at $\delta$ 5.04 ppm in the NMR spectra exhibited little overlap with the broad signal compared to the other peaks of *myo*-$IP_6$. Some slight overlap between the C2 peak of *myo*-$IP_6$ and the base of the orthophosphate peak was observed in soils S4 and S5.

## 3.3. Spike recoveries of total *myo*-$IP_6$

Spiking the soil extracts with *myo*-$IP_6$ resulted in a clear increase in its peak intensities at $\delta$ 5.04 ppm, 4.10 ppm, 3.72 ppm and 3.61 ppm across all soils (Fig. 2). On average, the increase in peak intensity of *myo*-$IP_6$ was 3-fold relative to the unspiked samples in terms of absolute intensity from the peak maximum to the baseline of the spectrum. The exception was sample S2, where the increase of the C1,3 and the C4,6 peak was 7-fold relative to the unspiked sample. The increase in peak intensity due to spiking varied for the four individual peaks of *myo*-$IP_6$. The C2 peak showed the greatest increase of intensity (3.2-fold) whereas the C5 peak showed the least (2.6-fold). The addition of the phytate standard to the soil extract also resulted in an increase in the intensity of other peaks to that of *myo*-$IP_6$, particularly peaks at $\delta$ 3.98, 4.14, 4.17 and 4.57 ppm.

The recovery of total *myo*-$IP_6$ in the six soil extracts using the SDF procedure with a broad signal was on average 95%, whereas this was on average 122% using the SDF procedure without a broad signal (Table 4). In addition, the variation in recovery of *myo*-$IP_6$ across the six samples was least using the former approach (SD of 5) compared to the latter approach (SD of 32).

## 3.4. Spike recoveries of individual peaks of *myo*-$IP_6$

Spike recoveries for each of the four peaks of *myo*-$IP_6$ differed between the SDF approaches across all soils (Table 4). Overestimation of spike recoveries using the SDF procedure without a broad peak was greatest (up to 213%) for the C5 peak of *myo*-$IP_6$ compared to all other peaks. Furthermore, spike recoveries of the C1,3 and C4,6 peaks of *myo*-$IP_6$ were overestimated on average 8% more than that of the C2 peak. The peak ratios of *myo*-$IP_6$ in the unspiked soils were on average 1.0 : 2.2 : 1.8 : 0.9 with a broad signal and 1.0 : 2.1 : 1.9 : 0.7 without a broad signal, when the C2 peak was set to 1 (soil S2 was not included due to unreliable measures of the C2 and C5 peaks of *myo*-$IP_6$).

## 3.5. Quantification of *myo*-$IP_6$ (and the broad signal) in soil extracts

Concentrations of total *myo*-$IP_6$ in soil extracts obtained with SDF with a broad peak ranged from 0.6 to 90.4 mg P per $kg_{soil}$, which comprised between 1% and 23% of total phosphomonoesters (Table 5). On average, the broad signal accounted for 64% of total phosphomonoesters across all soils (Table 5).

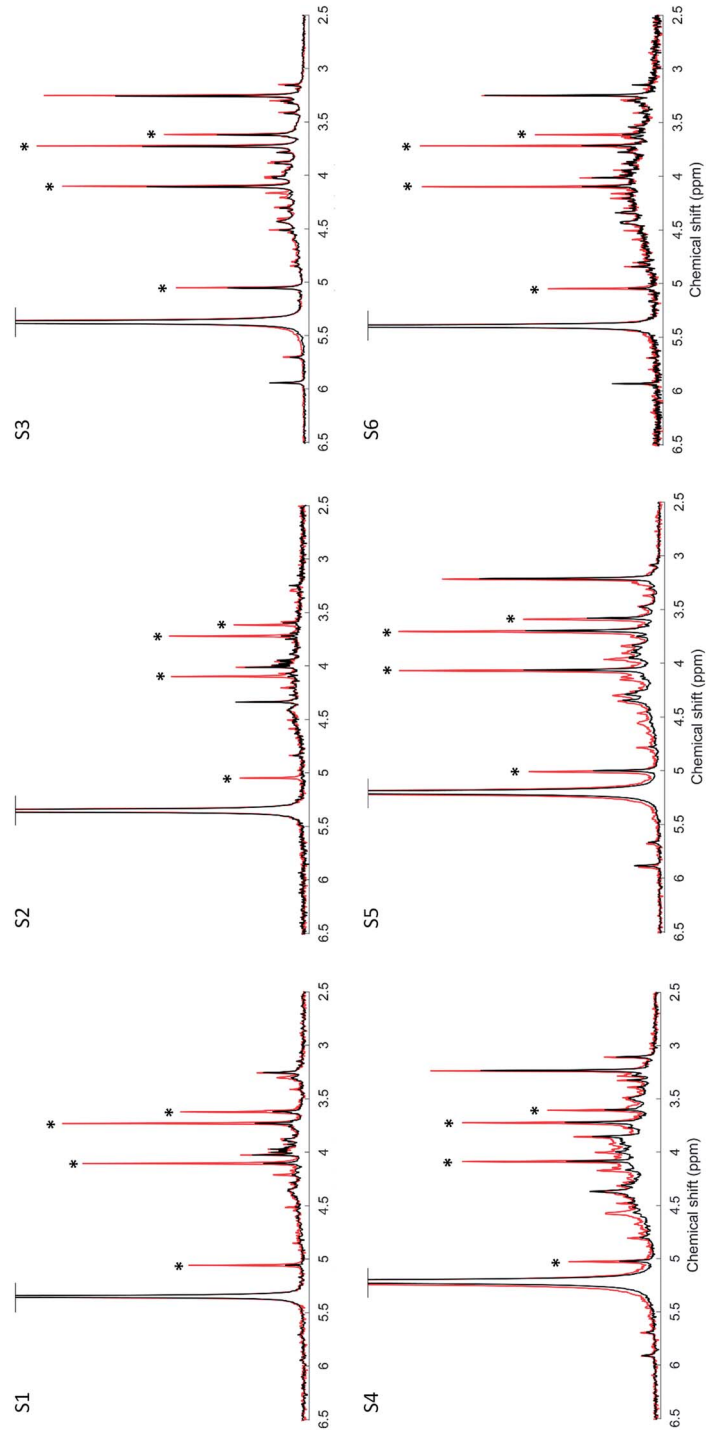


Fig. 2 Solution $^{31}$P nuclear magnetic resonance (NMR) spectra of the orthophosphate and phosphomonoester region on unspiked (black) and spiked (red) 0.25 M NaOH + 0.05 M EDTA soil extracts. Samples were spiked with a 10 μL aliquot of 5.5 mm *myo*-$IP_6$ (Sigma-Aldrich, product no. P5681) except for soil sample S5, which was spiked with a 11 mm *myo*-$IP_6$-standard solution. Signal intensities were normalized to the MDP peak intensity for direct comparison of unspiked and spiked extracts. However, in order to highlight spectral features, the vertical axes of the spectra have been increased by a factor of 1.7 for soils S3, S4 and S5, and by a factor of 10 for soils S1, S2 and S6. The four peaks generated by *myo*-$IP_6$ are marked with an asterisk.

Table 4 Calculated recoveries of the added *myo*-$IP_6$ (Sigma-Aldrich, product no. P5681) in 0.25 M NaOH + 0.05 M EDTA soil extracts across 6 soil samples, and their standard deviation (SD). Concentrations of the added *myo*-$IP_6$ were obtained from solution $^{31}$P NMR spectra using two spectral deconvolution fitting (SDF) procedures; one (i) with a broad underlying signal based on the method of Bünemann *et al.*, (2008),[12] and (ii) one without an underlying broad signal based on the method of Turner *et al.*, (2003).[10] The carbon nuclei C1–C6 of the inositol ring on which the phosphate group is attached has been indicated

| SDF procedure | *myo*-$IP_6$ | S1 (%) | S2 (%) | S3 (%) | S4 (%) | S5 (%) | S6 (%) | Average (%) | SD |
|---|---|---|---|---|---|---|---|---|---|
| With broad signal | Total *myo*-$IP_6$ | 96 | 90 | 99 | 92 | 91 | 105 | 95 | 5 |
| | C2-*myo*-$IP_6$ | 103 | 101 | 73 | 106 | 95 | 104 | 97 | 12 |
| | C1,C3-*myo*-$IP_6$ | 97 | 91 | 108 | 74 | 81 | 106 | 93 | 14 |
| | C4,C6-*myo*-$IP_6$ | 103 | 91 | 103 | 96 | 97 | 116 | 101 | 9 |
| | C5-*myo*-$IP_6$ | 73 | 77 | 96 | 106 | 95 | 81 | 88 | 13 |
| Without broad signal | Total *myo*-$IP_6$ | 146 | 120 | 73 | 151 | 94 | 147 | 122 | 32 |
| | C2-*myo*-$IP_6$ | 146 | 113 | 76 | 111 | 101 | 119 | 111 | 23 |
| | C1,C3-*myo*-$IP_6$ | 148 | 109 | 77 | 130 | 83 | 175 | 120 | 38 |
| | C4,C6-*myo*-$IP_6$ | 150 | 127 | 67 | 158 | 91 | 124 | 120 | 35 |
| | C5-*myo*-$IP_6$ | 135 | 133 | 76 | 213 | 117 | 167 | 140 | 46 |

When concentrations of *myo*-$IP_6$ as determined by SDF with a broad peak were subtracted from the *myo*-$IP_6$ values obtained by SDF without a broad peak, the amount of $P_{org}$ that would have been previously attributed to *myo*-$IP_6$ ranged from 1.3 to 56.1 mg P per $kg_{soil}$.

# 4. Discussion

## 4.1. Extractability of soil organic P and solution $^{31}$P NMR spectra

Concentrations of $P_{org}$ in NaOH-EDTA extracts were similar to reported values in previous studies.[19,37] The difference between total soil P as measured by XRF and NaOH-EDTA extractable P is likely due to $P_{inorg}$ held within mineral silicates and other insoluble mineral phases containing P.[40] Organic P extracted with the NaOH-EDTA technique is strongly correlated to pools of soil $P_{org}$.[40] The extraction method allows for detailed characterization of $P_{org}$ forms using $^{31}$P NMR spectroscopy.[8] Solution $^{31}$P NMR spectra were highly resolved and exhibited a high signal-to-noise ratio across all samples. The broad classes of P detected by NMR across all soils were phosphonates, orthophosphate, phosphomonoesters, phosphodiesters and pyrophosphate, except for the absence of phosphonates in S5 and phosphodiesters in S2. Their distribution within the total NMR signal is consistent with previous studies, which typically show the majority of NMR signal occurs in the orthophosphate and phosphomonoester region.[14,19,41] The peaks of *myo*-$IP_6$ were also clearly observed within this region, and therefore allowed for their quantification using SDF.[9]

## 4.2. Recovery of *myo*-$IP_6$ in soil extracts

Concentrations of added *myo*-$IP_6$ were overestimated when the SDF procedure did not include a broad signal. The reason for this is likely twofold: (1) the intensities of the *myo*-$IP_6$ peaks are higher when a broad signal is not included; and (2) the linewidths of these peaks when fitted to the baseline are greater if a broad signal is not included in the SDF compared to that when a broad signal is included. Therefore, the peak area belonging to compounds other than *myo*-$IP_6$ is being attributed to *myo*-$IP_6$, which may result in an overestimation of its concentration in soil. This supports the finding of Doolette *et al.*, (2010)[15] who reported an overestimation of a phytate spike by 54% when a broad signal was not fitted. Whilst the finding of Doolette *et al.*, (2010)[15] was higher than that found in the current study, it is likely due to a greater overlap among sharp peaks in the phosphomonoester region. The authors observed and fitted up to six sharp peaks in the orthophosphate and phosphomonoester region, but the C2 peak of *myo*-$IP_6$ was not visible because it overlapped with orthophosphate. This was not the case in the current study where all four peaks of *myo*-$IP_6$ were visible and the C2 peak of *myo*-$IP_6$ was clearly separated from orthophosphate.

Whilst the recovery of added *myo*-$IP_6$ was generally overestimated using SDF without a broad signal across all soils, this was not the case for soil S3. The reason for this is unclear but might be due to the high proportion of *myo*-$IP_6$ to total phosphomonoesters in this soil. It might also be due to an underestimation of the side regions at the base of the peak, as the fitting

Table 5 Concentrations of organic P compounds obtained from solution $^{31}$P NMR spectra of 0.25 M NaOH + 0.05 M EDTA soil extracts. The spectral deconvolution fitting of the phosphomonoester region has been carried out with the inclusion of an underlying broad signal

| Parameter | Unit | S1 | S2 | S3 | S4 | S5 | S6 |
|---|---|---|---|---|---|---|---|
| *myo*-$IP_6$ | mg P per $kg_{soil}$ | 4.4 | 0.6 | 80.7 | 46.2 | 90.4 | 6.3 |
| Proportion of *myo*-$IP_6$ to total phosphomonoesters | % | 12.0 | 1.0 | 23.0 | 9.0 | 23.0 | 4.0 |
| Broad peak | mg P per $kg_{soil}$ | 21.6 | 30.9 | 186.0 | 305.8 | 216.7 | 110.3 |
| Proportion of broad peak to total phosphomonoesters | % | 59.0 | 79.0 | 53.0 | 61.0 | 54.0 | 78.0 |

of neighbouring sharp peaks can influence the partitioning of signals within a particular region. In comparison to SDF with a broad signal of this soil, the fitting of side peak areas of *myo*-$IP_6$ appeared to improve based on a visual assessment, *i.e.* the peak height was reduced but the linewidth at half height increased. This highlights the sensitivity of peak fitting to small changes in peak shape for the quantification of P species in some soils.

The variability between the two SDF approaches differed in their recovery of added *myo*-$IP_6$ across all soils, which was least for the SDF approach with a broad signal than that without. The reason for this appears to be the relative proportion of the underlying broad signal to the *myo*-$IP_6$ peaks among different soils. This is consistent with other compounds that are present within this region, which overlay the broad signal. Doolette *et al.*, (2010)[15] reported that concentrations of glycerophosphate were doubled when SDF was carried out without an underlying broad signal. Of course, since *myo*-$IP_6$ exhibits 4 peaks in a NMR spectrum, this would vary between the individual peaks of *myo*-$IP_6$, based on differing proportions of an underlying broad signal.

Individual recoveries of the four peaks of *myo*-$IP_6$ differed. The greatest difference in the recovery of peaks from *myo*-$IP_6$ occurred when SDF was carried out without a broad signal, which supports that the baseline of the spectra varies within these chemical shifts.[9] The C1,3 and C4,6 peaks of *myo*-$IP_6$ have chemical shifts within the phosphomonoester region where the intensity of the broad peak is high relative to that for the C2 and C5 peaks. However, the recovery of the C5 peak of *myo*-$IP_6$ at $\delta$ 3.61 ppm was generally overestimated more than that of the other *myo*-$IP_6$ peaks. The C5 peak of *myo*-$IP_6$ is present on the shoulder of the broad signal, which has a maximum intensity at about $\delta$ 4.06 ppm. Doolette and Smernik (2015)[9] hypothesized that fitting peaks from the peak maxima to the baseline would result in substantially more signal from an underlying broad peak to the C5 peak of *myo*-$IP_6$ compared to the C2 peak of *myo*-$IP_6$. Moreover, the C5 peak appears to be most sensitive to changes in the fitting procedures, as it shows the highest variation for both deconvolution approaches. Another source of variation in the quantification of the C5 peak is that it overlaps with the base of the upfield C4,6 peak of *myo*-$IP_6$, and possibly peaks from uridine-2′-monophosphate, adenosine-2′-diphosphate, and some unidentified compounds.[33] There is also evidence that the broad peak itself is comprised of more than one component,[9,13] which may result in an imperfect Lorentzian/Gaussian distribution within the phosphomonoester region. Nevertheless, our study shows that the quantification of *myo*-$IP_6$ using SDF with a broad signal generally results in measures of *myo*-$IP_6$ that are more accurate and consistent across a diversity of soils compared to that of SDF without a broad signal.

The comparison of the peak ratios to the theoretical value of 1 : 2 : 2 : 1 was used in previous studies to evaluate the accuracy of the applied SDF procedure.[42] In our study, the peak ratios of *myo*-$IP_6$ were similar between the two SDF approaches and close to the theoretical ratio of 1 : 2 : 2 : 1.[43] Therefore, the ratio of peaks from *myo*-$IP_6$ cannot be used to assess the efficacy of the SDF for accurate quantification of organic P compounds. Since the peak ratios of *myo*-$IP_6$ were not a useful assessment of the SDF approaches, it is likely that other organic P compounds exhibiting sharp signals may provide some insight on the validity of the SDF approach. In particular, an overestimation would be likely for the C2,5 peak of *neo*-$IP_6$ in the 4-eq/2-ax conformation,[3] since its chemical shift is present in the region of the broad peak. Whereas the C1,3,4,6 peak of *neo*-$IP_6$ is located upfield of the orthophosphate peak and therefore does not overlap with the broad signal. We identified both of these peaks ($\delta$ 5.92 and 3.78 ppm) through spiking in soils S3, S4, S5 and S6 (data not shown), calculated their ratios, and compared to the theoretical ratio of 4 : 2.[3] Calculated ratios were on average 4.0 : 6.2 when carrying out SDF without a broad signal and 4.0 : 1.5 with an underlying broad signal. These results provide supporting evidence that a broad signal should be included when carrying out SDF.

In the current study, there was a large number of sharp peaks detected in the phosphomonoester region, which was likely due to optimized extraction techniques and high resolution NMR.[8] Interestingly, the intensity of several unidentified sharp peaks increased when the *myo*-$IP_6$ standard was added (Fig. 2). The *myo*-$IP_6$ standard contained many phosphomonoester impurities (see Fig. SI-2 in the ESI†), which are likely those of lower order *myo*-IPs.[44] Doolette and Smernik (2018)[44] investigated the chemical composition of a variety of purchased or synthesized phytate standards using solution $^{31}$P NMR spectroscopy. The authors found that the majority of phytate standards were impure and contained a mixture of lower- (and higher-) order IP, and orthophosphate. The authors suggested that thermal degradation during storage was the primary mechanisms in the degradation of higher-order IP to lower-order IP. This suggests the presence of lower order IP in soil extracts that could be detected using solution $^{31}$P NMR spectroscopy.

### 4.3. Concentrations of *myo*-$IP_6$ (and the broad signal) in soil

Our results demonstrate that a quantitative determination of *myo*-$IP_6$ in soil extracts using solution $^{31}$P NMR spectroscopy requires SDF procedures that include an underlying broad signal. In the current study, concentrations of *myo*-$IP_6$ and their proportion to the total pool of $P_{org}$ in soil were generally in range or lower than that more broadly reported in the literature. This most likely reflects the majority of published studies that primarily carry out SDF without a broad signal. Clearly, pools of *myo*-$IP_6$ in soil are an important portion of the soil $P_{org}$, which are found in the majority of soils across the world.[45] However, they do not account for the majority of $P_{org}$ in soil and sometimes found at negligible concentrations in some soils.[46–48]

The largest pool of soil $P_{org}$ was that of the broad signal across all soils. This is consistent with previous studies, where it generally comprises 40–70% of the total $P_{org}$ in soil.[14,16,19] The exact chemical nature of this pool remains unclear but can be described as phosphomonoesters in the form of large molecular structures,[14] which contain pools of $P_{org}$ resistant to enzymatic hydrolysis,[19] associated with humic fractions,[49] and are structurally complex.[13] The presence of a broad peak is consistent with previous studies using non-NMR techniques that report a large proportion of the $P_{org}$ in soil is unresolved and can occur in large molecular weight fractions.[2,28,48,50]

 

## 5. Conclusion

*myo*-Inositol hexakisphosphate is an important pool of soil organic P. However, its accurate quantification using solution $^{31}$P NMR spectroscopy followed by SDF is uncertain. Our aim was to compare the recovery of added *myo*-$IP_6$ using two SDF procedures in NMR spectra on soil extracts. The average recovery of total added *myo*-$IP_6$ by SDF with a broad signal was close to 100% and exhibited less variation than that by SDF without a broad signal. The recovery of individual peaks of *myo*-$IP_6$ differed between its four peaks, which was overestimated for the C5 phosphate peak by up to 140% when a broad peak was not fitted. We recommend that the accurate quantification of *myo*-$IP_6$ using solution $^{31}$P NMR spectroscopy on soil extracts includes a broad signal when carrying out SDF. This is also relevant for other sharp signals in the phosphomonoester region, which overlay the broad signal. Furthermore, our results show that previous studies reporting concentrations of *myo*-$IP_6$ using SDF without an underlying broad signal may be unreliable. It is essential that pools of *myo*-$IP_6$ (and the broad signal) are accurately determined for an improved understanding of the abundance and cycling of organic P in soil.

## Conflicts of interest

There are no conflicts of interest to declare.

## Acknowledgements

The authors kindly thank Dr Laurie Paule Mauclaire Schönholzer, Dr Federica Tamburini, Mr Björn Studer, Ms Monika Macsai, and Dr Charles Brearley for their technical support. Furthermore, the authors are grateful to Dr Astrid Oberson, Dr David Lester, Dr Chiara Pistocchi and Dr Gregor Meyer for providing soil samples. The authors are very thankful for the use of the D-*chiro*- and *neo*-$IP_6$ standards originating from the Dr Dennis Cosgrove collection and the Dr Max Tate collection, respectively. Funding from the Swiss National Science Foundation [grant number 200021_169256] is gratefully acknowledged.

## References

1 G. Anderson, in *The role of phosphorus in agriculture*, ed. F. E. Khasawneh, E. C. Sample and E. J. Kamprath, American Society of Agronomy, Crop Science Society of America, Soil Science Society of America, Madison, WI, 1980, pp. 411–431, DOI: 10.2134/1980.roleofphosphorus.c16.

2 H. F. Harrison, *Soil organic phosphorus a review of world literature*, CAB International, Wallingford, 1987.

3 B. L. Turner, A. W. Cheesman, H. Y. Godage, A. M. Riley and B. V. Potter, Determination of neo- and D-chiro-inositol hexakisphosphate in soils by solution $^{31}$P NMR spectroscopy, *Environ. Sci. Technol.*, 2012, **46**, 4994–5002.

4 G. C. J. Irving and D. J. Cosgrove, The use of gas-liquid chromatography to determine the proportions of inositol isomers present as pentakis- and hexakisphosphates in alkaline extracts of soils, *Commun. Soil Sci. Plant Anal.*, 1982, **13**, 957–967.

5 T. I. McLaren, R. J. Smernik, M. J. McLaughlin, A. L. Doolette, A. E. Richardson and E. Frossard, in *Advances in Agronomy*, ed. D. L. Sparks, Academic Press, 2020, vol. 160, pp. 51–124.

6 M. Ognalaga, E. Frossard and F. Thomas, Glucose-1-phosphate and myo-inositol hexaphosphate adsorption mechanisms on goethite, *Soil Sci. Soc. Am. J.*, 1994, **58**, 332–337.

7 R. H. Newman and K. R. Tate, Soil phosphorus characterisation by $^{31}$P nuclear magnetic resonance, *Commun. Soil Sci. Plant Anal.*, 1980, **11**, 835–842.

8 B. Cade-Menun and C. W. Liu, Solution phosphorus-31 nuclear magnetic resonance spectroscopy of soils from 2005 to 2013: a review of sample preparation and experimental parameters, *Soil Sci. Soc. Am. J.*, 2014, **78**, 19–37.

9 A. L. Doolette and R. J. Smernik, Quantitative analysis of $^{31}$P NMR spectra of soil extracts – dealing with overlap of broad and sharp signals, *Magn. Reson. Chem.*, 2015, **53**, 679–685.

10 B. L. Turner, N. Mahieu and L. M. Condron, Quantification of myo-inositol hexakisphosphate in alkaline soil extracts by solution $^{31}$P spectroscopy and spectral deconvolution, *Soil Sci.*, 2003, **168**, 469–478.

11 J. E. Hill and B. J. Cade-Menun, Phosphorus-31 nuclear magnetic resonance spectroscopy transect study of poultry operations on the Delmarva Peninsula, *J. Environ. Qual.*, 2009, **38**, 130–138.

12 E. K. Bünemann, R. J. Smernik, P. Marschner and A. M. McNeill, Microbial synthesis of organic and condensed forms of phosphorus in acid and calcareous soils, *Soil Biol. Biochem.*, 2008, **40**, 932–946.

13 T. I. McLaren, R. Verel and E. Frossard, The structural composition of soil phosphomonoesters as determined by solution $^{31}$P NMR spectroscopy and transverse relaxation (T2) experiments, *Geoderma*, 2019, **345**, 31–37.

14 T. I. McLaren, R. J. Smernik, M. J. McLaughlin, T. M. McBeath, J. K. Kirby, R. J. Simpson, C. N. Guppy, A. L. Doolette and A. E. Richardson, Complex forms of soil organic phosphorus – a major component of soil phosphorus, *Environ. Sci. Technol.*, 2015, **49**, 13238–13245.

15 A. L. Doolette, R. J. Smernik and W. J. Dougherty, Rapid decomposition of phytate applied to a calcareous soil demonstrated by a solution $^{31}$P NMR study, *Eur. J. Soil Sci.*, 2010, **61**, 563–575.

16 A. L. Doolette, R. J. Smernik and W. J. Dougherty, Overestimation of the importance of phytate in NaOH-EDTA soil extracts as assessed by $^{31}$P NMR analyses, *Org. Geochem.*, 2011, **42**, 955–964.

17 E. K. Bünemann, R. J. Smernik, A. L. Doolette, P. Marschner, R. Stonor, S. A. Wakelin and A. M. McNeill, Forms of phosphorus in bacteria and fungi isolated from two Australian soils, *Soil Biol. Biochem.*, 2008, **40**, 1908–1915.

18 S. R. Noack, M. J. McLaughlin, R. J. Smernik, T. M. McBeath and R. D. Armstrong, Crop residue phosphorus: speciation and potential bio-availability, *Plant Soil*, 2012, **359**, 375–385.

19 K. A. Jarosch, A. L. Doolette, R. J. Smernik, F. Tamburini, E. Frossard and E. K. Bünemann, Characterisation of soil organic phosphorus in NaOH-EDTA extracts: a comparison of $^{31}$P NMR spectroscopy and enzyme addition assays, *Soil Biol. Biochem.*, 2015, **91**, 298–309.

20 FAO and I. W. Group, *World reference base for soil resources 2014*, Food and Agriculture Organization of the United Nations FAO, Rome, 2014.

21 S. Bühler, A. Oberson, S. Sinaj, D. K. Friesen and E. Frossard, Isotope methods for assessing plant available phosphorus in acid tropical soils, *Eur. J. Soil Sci.*, 2003, **54**, 605–616.

22 E. K. Bünemann, S. Augstburger and E. Frossard, Dominance of either physicochemical or biological phosphorus cycling processes in temperate forest soils of contrasting phosphate availability, *Soil Biol. Biochem.*, 2016, **101**, 85–95.

23 G. Meyer, E. K. Bünemann, E. Frossard, M. Maurhofer, P. Mäder and A. Oberson, Gross phosphorus fluxes in a calcareous soil inoculated with Pseudomonas protegens CHA0 revealed by $^{33}$P isotopic dilution, *Soil Biol. Biochem.*, 2017, **104**, 81–94.

24 W. M. H. Saunders and E. G. Williams, Observation on the determination of total organic phosphorus in soils, *J. Soil Sci.*, 1955, **6**, 254–267.

25 S. Kuo, in *Methods of soil analysis part 3—Chemical methods*, ed. D. L. Sparks, A. L. Page, P. A. Helmke and R. H. Loeppert, Soil Science Society of America, American Society of Agronomy, Madison, WI, 1996, pp. 869–919, DOI: 10.2136/sssabookser5.3.c32.

26 B. J. Cade-Menun, C. W. Liu, R. Nunlist and J. G. McColl, Soil and litter phosphorus-31 nuclear magnetic resonance spectroscopy, *J. Environ. Qual.*, 2002, **31**, 457–465.

27 T. Ohno and L. M. Zibilske, Determination of low concentrations of phosphorus in soil extracts using malachite green, *Soil Sci. Soc. Am. J.*, 1991, **55**, 892–895.

28 R. A. Bowman and J. O. Moir, Basic EDTA as an extractant for soil organic phosphorus, *Soil Sci. Soc. Am. J.*, 1993, **57**, 1516–1518.

29 M. D. R. Vaz, A. C. Edwards, C. A. Shand and M. Cresser, Determination of dissolved organic phosphorus in soil solutions by an improved automated photo-oxidation procedure, *Talanta*, 1992, **39**, 1479–1487.

30 A. G. Vincent, J. Vestergren, G. Gröbner, P. Persson, J. Schleucher and R. Giesler, Soil organic phosphorus transformations in a boreal forest chronosequence, *Plant Soil*, 2013, **367**, 149–162.

31 A. V. Spain, M. Tibbett, M. Ridd and T. I. McLaren, Phosphorus dynamics in a tropical forest soil restored after strip mining, *Plant Soil*, 2018, **427**, 105–123.

32 A. L. Doolette, R. J. Smernik and W. J. Dougherty, Spiking improved solution phosphorus-31 nuclear magnetic resonance identification of soil phosphorus compounds, *Soil Sci. Soc. Am. J.*, 2009, **73**, 919–927.

33 J. Vestergren, A. G. Vincent, M. Jansson, P. Persson, U. Ilstedt, G. Gröbner, R. Giesler and J. Schleucher, High-resolution characterization of organic phosphorus in soil extracts using 2D $^{1}$H–$^{31}$P NMR correlation spectroscopy, *Environ. Sci. Technol.*, 2012, **46**, 3950–3956.

34 M. I. Makarov, L. Haumaier and W. Zech, Nature of soil organic phosphorus: an assessment of peak assignments in the diester region of $^{31}$P NMR spectra, *Soil Biol. Biochem.*, 2002, **34**, 1467–1477.

35 B. L. Turner, N. Mahieu and L. M. Condron, Phosphorus-31 nuclear magnetic resonance spectral assignments of phosphorus compounds in soil NaOH-EDTA extracts, *Soil Sci. Soc. Am. J.*, 2003, **67**, 497–510.

36 R. L. Vold, J. S. Waugh, M. P. Klein and D. E. Phelps, Measurement of spin relaxation in complex systems, *J. Chem. Phys.*, 1968, **48**, 3831–3832.

37 B. L. Turner, Soil organic phosphorus in tropical forests: an assessment of the NaOH-EDTA extraction procedure for quantitative analysis by solution $^{31}$P NMR spectroscopy, *Eur. J. Soil Sci.*, 2008, **59**, 453–466.

38 B. L. Turner, N. Mahieu and L. M. Condron, The phosphorus composition of temperate pasture soils determined by NaOH-EDTA extraction and solution $^{31}$P NMR spectroscopy, *Org. Geochem.*, 2003, **34**, 1199–1210.

39 W. J. Dougherty, R. J. Smernik and D. J. Chittleborough, Application of spin counting to the solid-state $^{31}$P NMR analysis of pasture soils with varying phosphorus content, *Soil Sci. Soc. Am. J.*, 2005, **69**, 2058–2070.

40 T. I. McLaren, R. J. Simpson, M. J. McLaughlin, R. J. Smernik, T. M. McBeath, C. N. Guppy and A. E. Richardson, An assessment of various measures of soil phosphorus and the net accumulation of phosphorus in fertilized soils under pasture, *J. Plant Nutr. Soil Sci.*, 2015, **178**, 543–554.

41 A. L. Doolette, R. J. Smernik and W. J. Dougherty, A quantitative assessment of phosphorus forms in some Australian soils, *Soil Res.*, 2011, **49**, 152–165.

42 A. G. Vincent, J. Schleucher, G. Gröbner, J. Vestergren, P. Persson, M. Jansson and R. Giesler, Changes in organic phosphorus composition in boreal forest humus soils: the role of iron and aluminium, *Biogeochemistry*, 2012, **108**, 485–499.

43 A. J. R. Costello, T. Glonek and T. C. Myers, $^{31}$P nuclear magnetic resonance-pH titrations of myo-inositol hexaphosphate, *Carbohydr. Res.*, 1976, **46**, 159–171.

44 A. L. Doolette and R. J. Smernik, Facile decomposition of phytate in the solid-state: kinetics and decomposition pathways, *Phosphorus, Sulfur, Silicon Relat. Elem.*, 2018, **193**, 192–199.

45 B. L. Turner, M. J. Papházy, P. M. Haygarth and I. D. McKelvie, Inositol phosphates in the environment, *Philos. Trans. R. Soc. Lond. Ser. B Biol. Sci.*, 2002, **357**, 449.

46 B. L. Turner, Organic phosphorus in Madagascan rice soils, *Geoderma*, 2006, **136**, 279–288.

47 C. Williams and G. Anderson, Inositol phosphates in some Australian soils, *Soil Res.*, 1968, **6**, 121–130.

48 J. H. Steward and M. E. Tate, Gel chromatography of soil organic phosphorus, *J. Chromatogr. A*, 1971, **60**, 75–82.

49 Z. He, D. C. Olk and B. J. Cade-Menun, Forms and lability of phosphorus in humic acid fractions of Hord silt loam soil, *Soil Sci. Soc. Am. J.*, 2011, **75**, 1712–1722.

50 R. C. Dalai, in *Advances in Agronomy*, ed. N. C. Brady, Academic Press, 1977, vol. 29, pp. 83–117.

 